Method for the Generation of Broadband Acoustic Signals

Paul Swincer (1), Binh Nguyen (2) and Shane Wood (2)

(1) School of Electrical and Electronic Engineering, University of Adelaide, Adelaide, Australia
(2) Maritime Operations Division, Defence Science and Technology Organization, Edinburgh, Australia

ABSTRACT

Conventional active sonar systems use narrowband pulsed waveforms. It is suggested that using broadband acoustic pulses will exploit more details of the acoustic scattering from the target target, medium and the environment that will assist in the development of improved target detection and classification algorithms. Problems of generating broadband signals such as resonances, distortion and ripples have been studied by several researchers. In this paper, we explore several aspects of the problem including methods for equalisation of the amplifier and transducer used to transmit the pulses. Several approaches for equalising the received pulses are also examined.

INTRODUCTION

Active sonar involves the transmission of 'pulses' of sound into the underwater environment in order to gain information about the environment from the detected echoes or scattering of the sound from various underwater targets or objects. Historically these pulses were simply bursts of constant-frequency sinusoid used to determine the distance to the target; however it is possible that a wideband sonar signal may reveal more details of the acoustic scattering from the target, allowing us to classify it and separate it from 'false alarm' signals.

This paper outlines some research and methodology used to generate and transmit broadband sonar signals in the laboratory. There are several practical limitations in this experimental setup that makes broadband transmission more difficult. Firstly, the duration of the pulse that can be transmitted may be limited by factors such as power amplifier duty cycles, echoes and reverberations in the laboratory tank, or interference between the transmitted and received pulse in the case of a monostatic system. Secondly, and more importantly, the spectrum output of the amplifier and transducer are not flat, introducing variation into the transmitted signal. Unless this variation is known or corrected, it will be difficult to determine whether features of the received signal are due to the object itself or the measurement system, rendering the results unreliable.

In approaching the first problem, a pulse developed by Berkhout was used after considering several other types of broadband pulses in order to give maximum temporal resolution with minimum pulse length.

The second problem was approached in several different ways. The first method involved correcting the input signal for the distortion in the sonar transmitter so that the transmittted pulse was close to the desired waveform. The second approach involved correcting the received waveforms based on a standard calibration signal, such as the incident pulse or the reflection from a standard object such as a sphere.

Each of these approaches is tested on a well-characterized object to evaluate whether they have in fact improved the detail and temporal resolution in the measured output.

MEASUREMENT SYSTEM DESCRIPTION

Although many practical sonar applications occur in large bodies of water such as the ocean, a controlled laboratory test often provides more repeatable results. The wavelength of sonar used has been decreased so that scale models can be used as targets. A diagram describing the basic layout of the sonar system used to measure the sonar pulses transmitted in the water is given in figure 1.

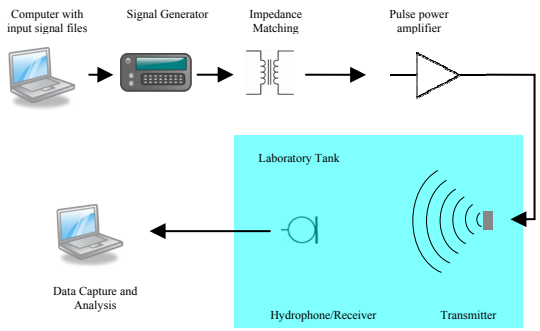

Figure 1. Test configuration for measuring incident signals

A similar test setup was used to measure the scattered signal from various objects placed at a distance from the transmitter. However in this case the configuration modelled a monostatic active sonar system, with an object placed at the location of the hydrophone in the diagram above. The scattered sonar signals from this object were measured by a hydrophone at the same location as the transmitter. By rotating the object through a number of different angles, a complete sonar 'fingerprint' of the object could be constructed. Our aim was to improve these measurements using suitable broadband sonar pulses.

BROADBAND SONAR SIGNALS

One of the first considerations when designing a broadband system is the type of broadband pulse to be transmitted. An ideal broadband signal should have a flat frequency spectrum over a finite range of frequencies, making calibration easier and ensuring that the acoustic response of the object can be measured accurately over the entire frequency range. They should have good stopband attenuation so that most of the transmitted power is present over the frequency range of interest. Finally they should be as short as possible in terms of time duration (Cobo 2002), as this results in better resolution of target detail. From a practical point of view short pulses also minimize the problem of reverberations and reflections contaminating the received signal, as these reflections could be removed by time gating.

We experimented with several different broadband pulses including a linear chirp (frequency-varying sinusoid) and a Butterworth pulse (the impulse response of a Butterworth filter). However the best results were obtained using Berkhout pulses.

Berkhout Pulses

According to research by Berkhout (Berkhout 1984), minimum-length broadband pulses have a zero phase spectrum and magnitude given by:

$$|X(f)| = \begin{cases} \cos^{\gamma} \dfrac{\pi(f - f_c)}{BW}, & f_1 \le f \le f_2 \\ 0, & \text{otherwise} \end{cases} \qquad (1)$$

where:

- f_1 is the minimum desired frequency
- f_2 is the maximum desired frequency
- BW is the bandwidth, $BW = f_2 - f_1$
- f_c is the centre frequency, $f_c = \dfrac{f_2 - f_1}{2}$
- γ is a trade-off factor which determines the degree of roll-off outside the desired frequency band as well as the flatness within the pass-band. γ is always a positive number, and the degree of roll-off becomes higher as γ approaches 0, while the pass-band spectrum becomes flatter.

An example of a Berkhout pulse is given in figure 2, with its magnitude frequency spectrum in figure 3. As with all broadband pulses, the rate at which the signal decays on each side of the main pulse decreases as the bandwidth of the pulse is decreased. This means that the power transmitted can be quite low, especially for very wideband pulses.

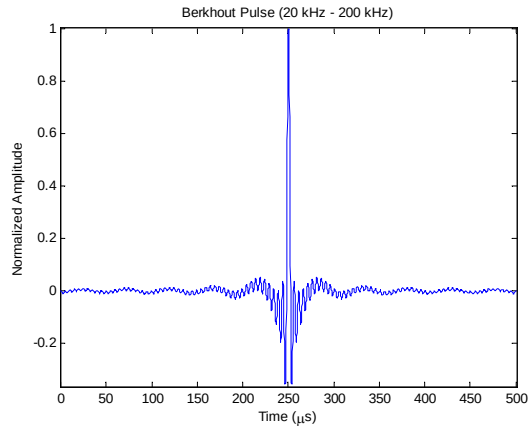

Figure 2. Example of a Berkhout pulse (γ = 0.01)

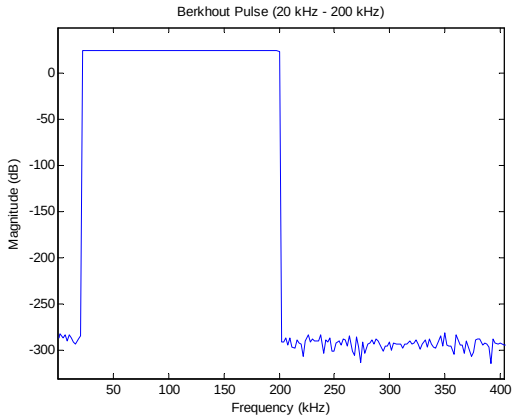

Figure 3. Spectrum of Berkhout Pulse (γ = 0.01)

TRANSMITTER SYSTEM FREQUENCY RESPONSE

Characterizing the frequency response of the sonar transmitting system is an important part of a useful wideband sonar system. Without accounting for the characteristics of the transmitter system in some way, we have no way of telling whether variations in the spectrum of the received signal are caused by the target or by the frequency response of the system.

The transmitter system typically consists of a number of components, including signal generator, power amplifier and sonar transmitter. To simplify analysis we combine all these components into a single 'black box' component with frequency response *H*(*f*), as shown in figure 4.

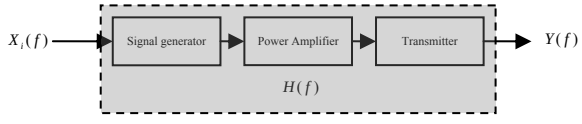

Figure 4. 'Black box' model of transmitter system

The frequency response of the system can simply be measured by sending an input signal with frequency spectrum *X*(*f*) into the system and measuring the frequency response of the output signal *Y*(*f*), as described in equation 2.

$$H(f) = \frac{Y(f)}{X(f)} \qquad (2)$$

In practice it is impossible to determine an accurate estimate of the frequency response using a measurement from a single input signal. It is necessary to ensure that sufficient input power is present at each frequency so that the response at that frequency can be reliably determined, given the presence of noise in the system and the fact that the transmitter frequency response may contain sharp nulls. In our transmitter system characterizations we chose to use a number of input signals which contained energy over a narrow finite band of frequencies. This allowed us to accurately measure the frequency response of the system over that frequency band. The frequency bands were chosen such that they overlapped each other to cover the entire frequency range of interest, and the results were combined to produce a single continuous estimate of the transfer function $H(f)$.

A plot of the resulting frequency response for one particular transmitter used is given in figure 5.

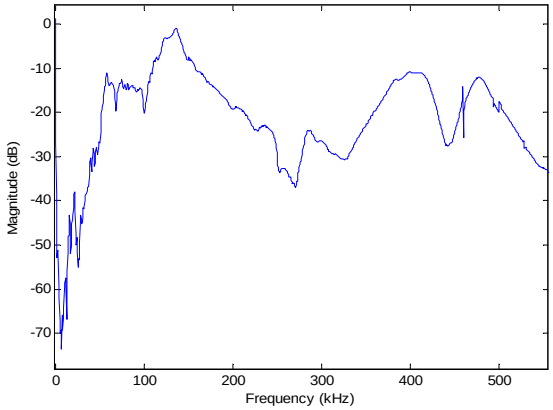

Figure 5. Frequency response of transmitter system

The results from this measurement show almost 50 dB of variation across the range 20 – 220 kHz. Most of this variation is due to the transmitter itself, which is designed with a strong resonant frequency. In addition, while the high-frequency part of the spectrum is relatively smooth, the response below 150 kHz contains many sharp crests and troughs, and was comparatively hard to equalize. In particular, at some frequencies, such as around 70 kHz, the frequency response fluctuated significantly each time the response was measured. This suggested that the system may be non-linear at these frequencies. A plot of the coherence of the transmitter frequency response measurements is given in figure 6. This shows a lack of coherence which could be due to several factors (Bendat 1980):

- Noise present in the system. This can particularly be a problem when the frequency response contains a deep null.
- External signals, such as interference picked up from local AM radio stations, can cause non-linearity. A noise filter can be implemented in many cases to remove this interference.
- Insufficient frequency resolution: for very sharp variations across the frequency response, the frequency resolution (frequency bin width) may be insufficient to accurately sample the frequency spectrum. This can be overcome by using longer test pulses and thus introducing more points into the FFT, but in our case this was impractical due to the reflections and reverberations which would contaminate the received signal.
- The system itself may be nonlinear to a certain extent.

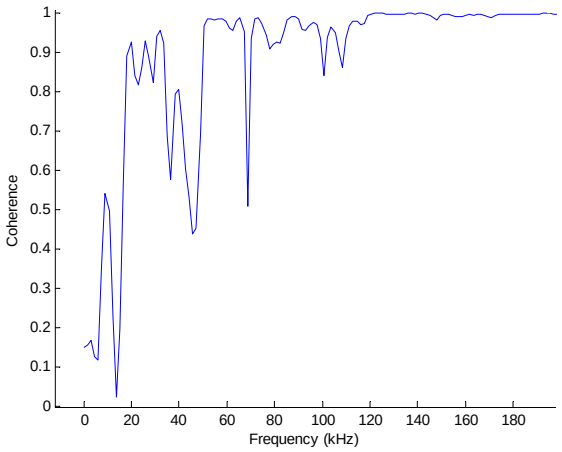

Figure 6. Coherence of frequency response measurements

In our case the non-linearity is most likely to be caused by the presence of noise contaminating the output signal when the response is low, combined with the presence of sharp nulls in the response. Avoiding a transmitter with such sharp nulls is thus an important consideration when designing a broadband sonar system.

TRANSMITTER SYSTEM RESPONSE EQUALISATION

At this stage we have an accurate measurement of the system frequency response $H(f)$. An input Berkhout pulse (80 – 220 kHz) with a flat frequency spectrum will be transmitted to the water as a sonar pulse with a very different spectrum, as shown in figure 7.

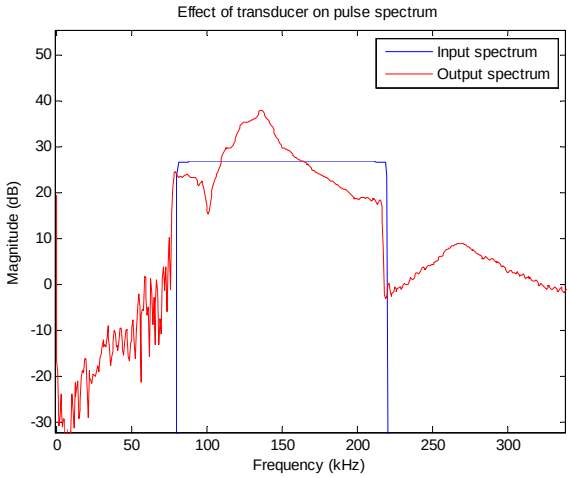

Figure 7. Effect of transmitting system on pulse

In the frequency domain, we can represent the spectrum of the output signal as the product of the spectrum of the input signal and the frequency response of the system:

$$Y_i(f) = X_i(f)H(f) \tag{3}$$

Now let us suppose that instead of specifying $x_i(t)$, we specify the output $y_p(t)$ to be the prescribed signal we wish to transmit as a sonar signal into the water. We need to then deter-

mine the input signal $x_p(t)$ we should transmit to produce this desired output. In the frequency domain, this is described by the following spectral division (inverse filtering) equation:

$$X_p(f) = \frac{X_i(f)}{H(f)} \tag{4}$$

In practice however there are problems with using equation 4 to derive the correct input signal. In particular, the value of $H(f)$ is extremely small at some frequencies due to the system having a poor response at some frequencies. This can cause instability due to the division process as any noise present in these parts of the spectrum has a disproportionately large effect on the output signal.

To avoid this problem, we introduce a small filter stabilization constant to the denominator (Cobo 1994):

$$X_p(f) = X_i(f).\frac{H^*(f)}{|H(f)|^2 + p^2} \tag{5}$$

The value of p needs to be chosen carefully. If it is too small, it will be ineffective in reducing instability as it will have a similar magnitude to the noise and error causing the instability; if it is too large, it will swamp the other denominator term and destroy the equalisation we are trying to achieve. A p value of about 0.0001 was found to be satisfactory in our experiments, although it was observed that smaller values of p produced better results at lower frequencies, while increasing the level of unwanted noise contaminating the corrected signal at higher frequencies.

This approach assumes that the noise power is constant at all frequencies. An alternative approach for non-flat noise spectrums is to use a Wiener filter which instead of using a constant value for p, uses a value based on the noise spectrum (Holly 1984). This approach was not actually used in our tests but is a potential idea for future research:

$$X_p(f) = X_i(f)\frac{H^*(f)S_x(f)}{|H(f)|^2 S_x(f) + S_u(f)} \tag{6}$$

where:

- $S_x(f)$ is the noise power spectrum
- $S_u(f)$ is the signal power spectrum

Using equation 5 the spectrum of the output pulse was 'flattened' significantly as a result of accounting for the frequency response of the transducer when transmitting the sonar pulse. Quantitatively, a variation of 27 dB in the spectrum of the output signal over a range of 140 kHz was reduced to 4 dB by this technique. This is illustrated in figure 8.

Figure 9 demonstrates equalisation in the time domain. The first plot illustrates an example of an ideal broadband pulse we desire to be transmitted. However the second plot shows the actual shape of this pulse after it has been distorted by the transmitter system. After equalizing the input signal for the frequency response of the system, we obtain the input pulse in the third plot, which, when transmitted into the system, produces a sonar pulse which matches very closely the desired waveform. This is illustrated in the fourth plot in figure 9.

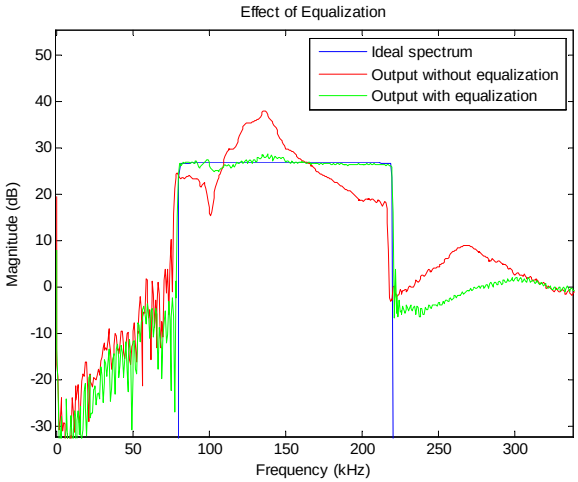

Figure 8. Correction of frequency spectrum

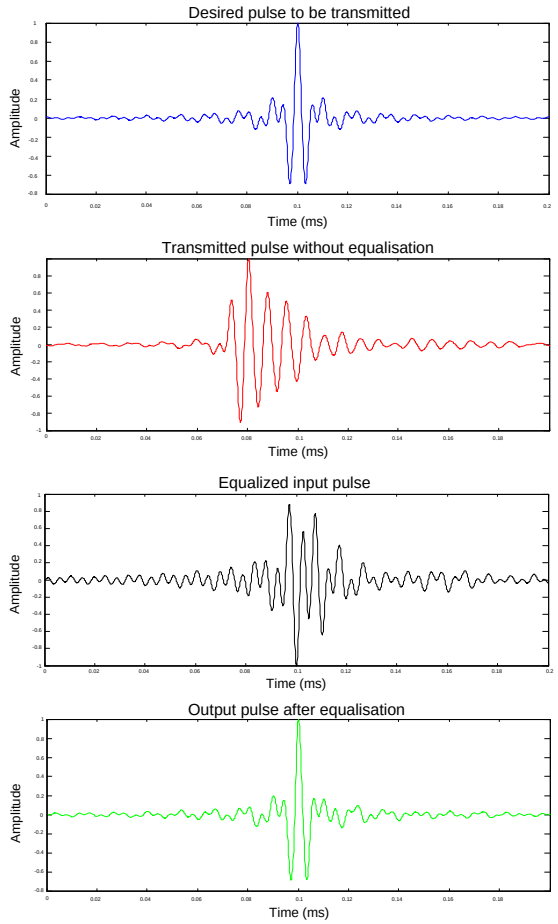

Figure 9. Equalisation in the time domain

SCATTERING MEASUREMENT RESULTS

At this point we examined whether this equalisation process actually provided us with more detail about an object when measurements of the scattered sonar signal from the object were made. The object chosen was an air-filled brass cylinder with one hemispherical end and a conical end, as illustrated in figure 10.

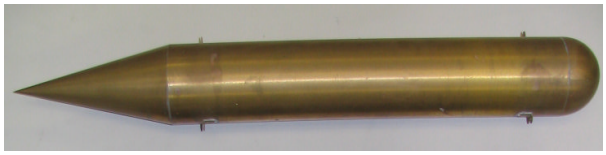

Figure 10. Air-filled brass cylinder

The object was rotated in the horizontal plane in one degree increments such that reflections from the sides, as well hemispherical and conical ends of the object could all be recorded. After making 360 such measurements at every angle in the horizontal plane around the object, three-dimensional plots of the intensity of the received scattered signal for each angle could be produced. The following plots show the difference in the received signals in the time domain when equalisation is applied.

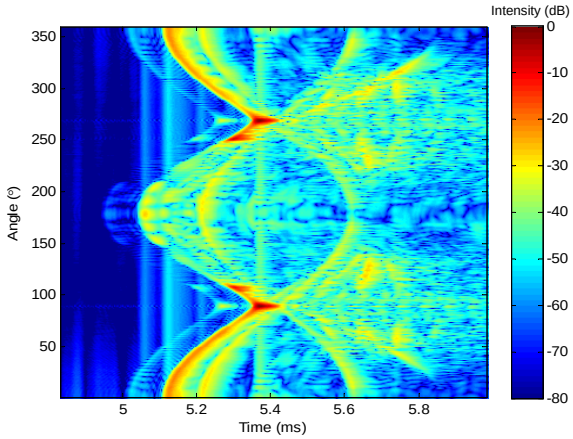

Figure 11. Acoustic scattering versus angle and time - unequalized input

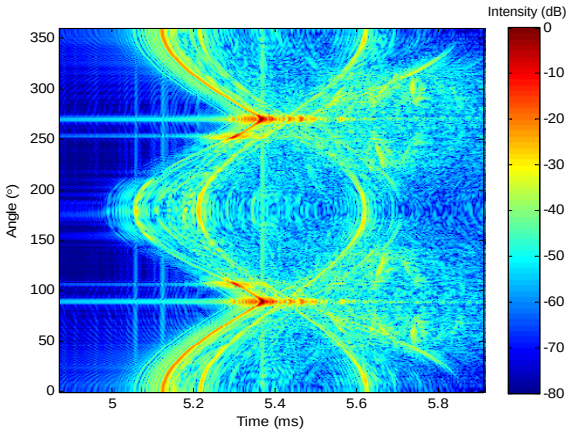

Figure 12. Acoustic scattering versus angle and time - equalized input

These plots reveal information about the physical geometry of the object, including the strong reflection from the sides at 90° and 270°, a constant strong reflection from the hemispherical end from 270° to 360° and 0° to 90°, and a weaker reflection from the conical end at 180°.

It can be seen that the angle versus time plot is significantly sharper and clearer in figure 12, when the input has been corrected for the frequency response of the system, than in figure 11 where no attempt has been made to compensate for the system's frequency response. This allows more precise identification of object scattering features with reduced uncertainty as to the exact time of the main reflections from key features. The second plot also contains significantly more detail than the unequalised results, which can be used to derive more information about the internal structure of the object.

An alternative method for analysing these results is to plot the scattering intensity versus frequency for each angle around the object. These results are plotted in figure 13 and figure 14.

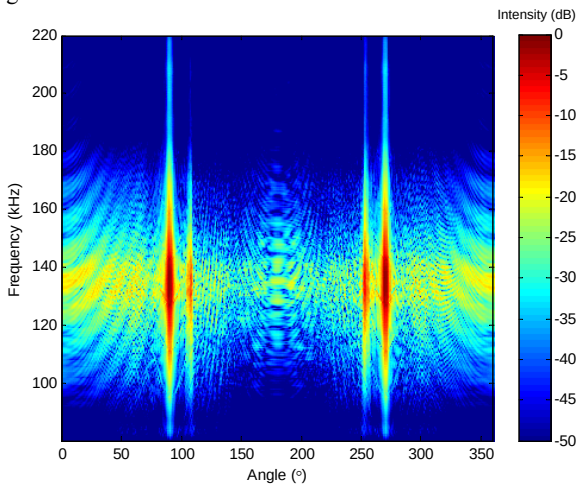

Figure 13. Acoustic scattering versus angle and frequency – no equalisation

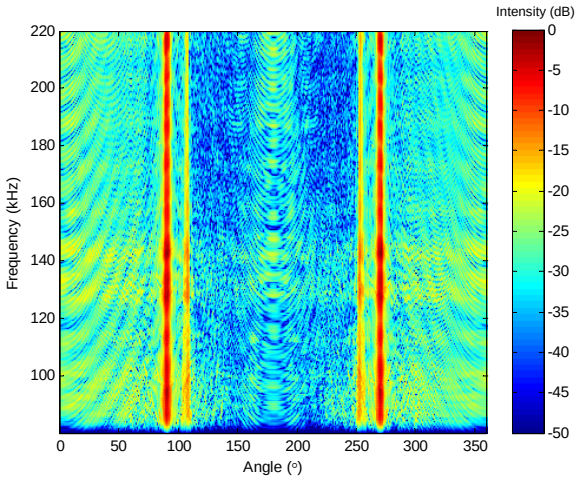

Figure 14. Acoustic scattering versus angle and frequency - with equalisation

In theory the specular reflection at 90° and 270° should be approximately constant at all frequencies. This is clearly not the case in the first plot when the input signal was not corrected for the transfer function of the system. However in the second plot the details are much clearer and the specular reflection is almost constant across all frequencies, as expected. The level of detail in the second plot – particularly at high and low frequencies, away from the resonant frequency of the transducer – is significantly higher than that of the first plot.

In conclusion, these results demonstrate that active sonar measurements can be significantly improved when the input signal is shaped to account for the frequency response of the transmitter system.

POST MEASUREMENT EQUALISATION

In some cases it is impractical or even impossible to measure the transmitter response before making measurements. Small variations in the transmitter frequency response can be easily introduced by changes in ambient temperature or changes to the system configuration such as the introduction of different equipment. The process of calibrating the transmitter frequency response can take some time, and consequently it may not be desirable to repeat this process every time a measurement must be made.

Consequently a simple method is required to perform the equalisation after measurements have been made. When making acoustic scattering measurements, two initial measurements on the system can easily be made to assist in subsequent data processing: a measurement of the incident pulse at the object position, and a measurement of the scattering from a reference object such as a stainless steel sphere located at the object position. Both approaches will be examined in subsequent sections.

Incident Pulse Equalisation

When an incident pulse with spectrum $X(f)$ is passed through an active sonar system with transmitter system frequency response $H(f)$, and where the effect of the object on the scattered signal can be modelled by $T(f)$, the spectrum of the output signal $Y(f)$ is given by the following relationship:

$$Y(f) = H(f)X(f)T(f) \tag{7}$$

Consequently to remove the effect of $H(f)$ we simply divide it out of the expression:

$$Y_{equalized}(f) = \frac{Y(f)}{H(f)} = X(f)T(f) \tag{8}$$

The actual implementation of this spectral division process, to handle nulls in $H(f)$ and avoid instability due to noise, has been discussed in a previous section.

To carry out this measurement we need an estimate of the frequency response $H(f)$. This can be obtained by simply transmitting a broadband pulse with response $X(f)$ and measuring the spectrum of the resulting sonar signal $Y(f)$ some distance from the transducer. This process assumes that the hydrophone used to perform the measurement has an ideally flat frequency response. Then the frequency response of the system can be calculated simply by dividing $Y(f)$ by $X(f)$.

To test this process we applied it to sonar scattering measurements of the brass cylinder object from the previous section. The results are shown in the following plots. Figure 15 shows that as a result of the strong resonance in the frequency response of the transmitter system, the specular reflection at 90° and 270° is not constant across all frequencies, as predicted by theory.

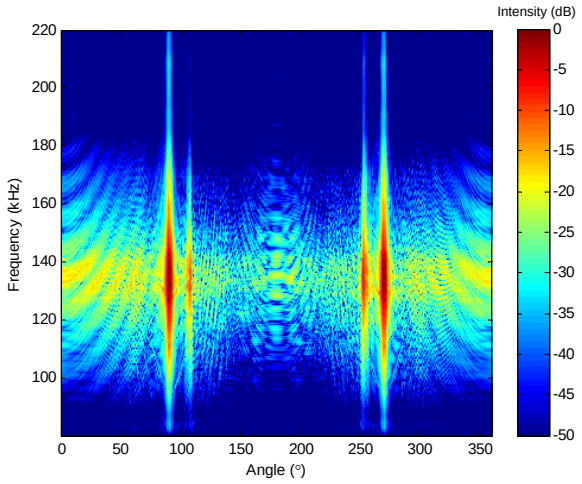

Figure 15. Acoustic scattering versus angle and frequency - no equalisation

Figure 19 shows the scattering results with equalisation applied. This plot clearly demonstrates an improvement in the quality of the measurements, and while the resonance has not been completely removed, its effect has been significantly reduced.

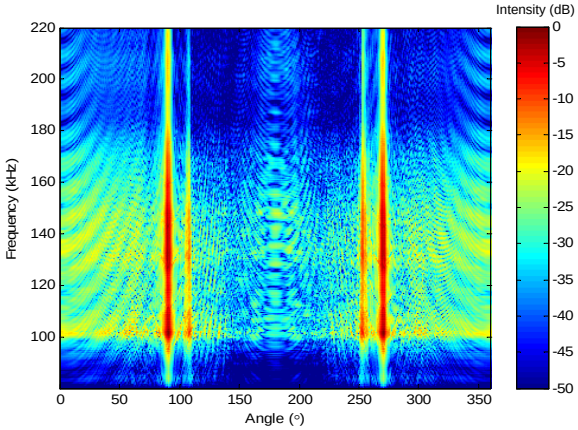

Figure 16. Acoustic scattering versus angle and frequency - with equalisation

While some improvement has been made to the quality of the output measurements by this technique, the results are not as impressive as those demonstrated in figure 14. This could be due to several factors. Firstly, only one measurement was used to determine $H(f)$, compared to the multiple measurements used in our first approach. Secondly, the input signal had not been corrected to account for the system frequency response, which meant that particular frequencies had not been amplified or attenuated to account for the nulls in the frequency response. These frequencies became contaminated with noise in the output measurements, and the output processing used had no way of dealing with this. Consequently the response is significantly weaker at higher and lower frequencies away from the resonant frequency.

Equalisation with a Standard Sphere

Using the acoustic scattering from a spherical object has long been a standard method for calibrating transmitter systems. Spherical objects are favoured as the impulse response of such a object can be analytically calculated accurately using physical laws. Consequently by comparing the measured reflection with the expected reflection from the sphere, the

frequency response of the system can be determined. This can be achieved using the following relationship:

$$Y(f) = X(f)H(f)F_{sphere}(f)$$
$$\therefore H(f) = \frac{Y(f)}{X(f)F_{sphere}(f)} \quad (9)$$

In order to apply this method, it is necessary to determine how the reflection from the sphere affects the frequency response, i.e. find $F_{sphere}(f)$. Due to diffraction around the sphere and sound resonances in the sphere itself, the frequency response is quite complex, as illustrated in figure 17 where the predicted frequency response of a 10 cm stainless steel sphere is displayed (Faran 1951).

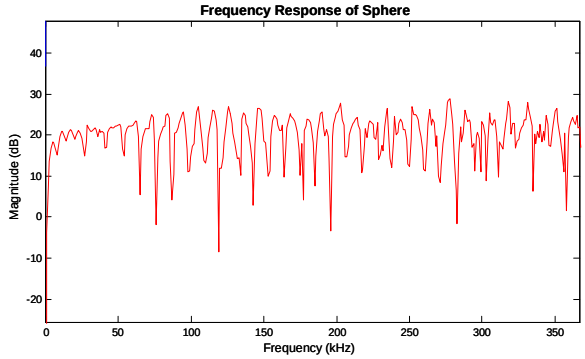

Figure 17. Frequency Response of Steel Sphere

The difficulty with using this response is that it contains many sharp peaks and nulls whose location is highly dependent upon the exact properties of the steel sphere. Any variations or imperfections in the sphere will shift the location of the nulls and render this theoretical prediction almost useless.

One way to avoid this problem (Dragonette 1981) is to realize that the impulse response of a sphere consists of two main components: the specular reflection of the sphere, which has an almost ideal flat broadband frequency response (assuming the sphere is rigid), followed by a train of echoes caused by diffraction and resonances in and around the sphere. This is illustrated by the impulse response in figure 18.

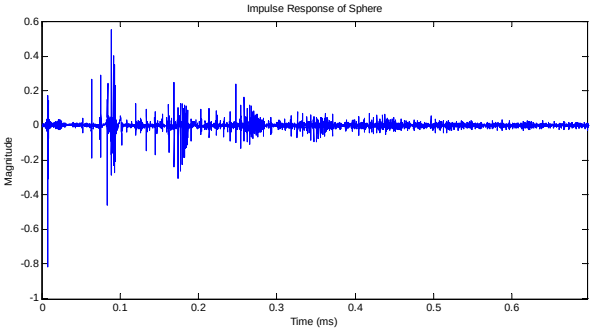

Figure 18. Impulse Response of Stainless Steel Sphere

Thus by isolating the first echo or specular reflection from the sphere from the following echoes caused by the sphere's elasticity, we can assume that the frequency response from the sphere is practically flat, and thus obtain a reasonable estimate of $H(f)$ from equation 9. In practice, however, the reflections from the different components of the spherical response overlap in time, as the input test signal $x(t)$ has some time duration. A signal processing technique (Stanton 2008) has been developed to overcome this problem and is outlined briefly as follows.

Firstly the output signal is correlated with the input signal.

$$\mathrm{cp}_1(t) = x(t) \otimes y(t) \quad (10)$$

In the frequency domain this becomes:

$$\mathrm{CP}_1(f) = X^*(f)Y(f) \quad (11)$$

A second compressed pulse can be generated which incorporates the impulse response of the sphere, as follows:

$$\mathrm{cp}_2(t) = \{f_{sphere}(t) * x(t)\} \otimes x(t) \quad (12)$$

Taking the Fourier transform of (12) gives:

$$\mathrm{CP}_2(f) = F_{sphere}(f)X(f)X^*(f) \quad (13)$$

Recall from (9) that the transfer function of the system is given by:

$$H(f) = \frac{Y(f)}{F_{sphere}(f)X(f)} \quad (14)$$

Multiplying both the numerator and denominator of this expression by $X^*(f)$, it can be seen that the frequency response of the system can be expressed as:

$$H(f) = \frac{\mathrm{CP}_1(f)}{\mathrm{CP}_2(f)} \quad (15)$$

Using this estimate of the frequency response, we were able to perform some correction of the scattering measurements from the object as shown in the following frequency versus angle plot.

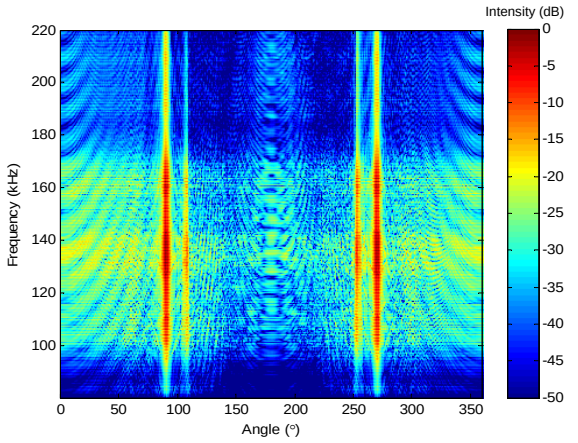

Figure 19. Acoustic scattering versus angle and frequency - after equalisation

By comparing this plot, which has been corrected with our transfer function estimate, with the original results (figure **13**), it can be observed that the equalisation process has improved the results. More details of the reflection pattern are

now observable at the higher and lower frequencies away from the resonant frequencies. Moreover the strength of the specular reflection at 90° and 270° is much less dependent upon frequency, showing closer agreement to theoretical results.

CONCLUSION

This paper has examined several different methods for generating broadband sonar signals. A suitable broadband signal type (the zero-phase pulses developed by Berkhout) was chosen for their superior scattering feature resolution properties. A key issue is then accounting for the non-flat frequency response of the transmitter system, and several techniques were developed to do this.

The best technique involves taking a number of measurements to carefully measure the frequency response of the system. This measured frequency response can then be used to equalize the input signal using a spectral division process, such that the output sonar signal matches the desired signal. Instability in the spectral division was addressed in several ways, including using a small positive constant in the denominator as trialled by Cobo (Cobo 1994), as well as a Wiener filter, as trialled by Holly (Holly 1984). This equalisation was largely successful, reducing a variation of 25 dB to less than 4 dB over a bandwidth of 140 kHz in the output signal.

Research and experimentation was also carried out into several other ways to estimate the frequency response of the transmitter system using a single measurement. One such method used a measurement of the transmitted pulse at some distance from the sonar transmitter, while an alternative method involved using the reflection from a standardized sphere. Both methods produced reasonable results, although inferior to the results obtained using the first technique.

Future research could involve studies of alternative spectral division processes (such as Tikhonov regulation) (Kaipio 2005); development of better broadband sonar transmitters with a flatter frequency response; and developing hardware that can perform the correction automatically in real time.

REFERENCES

Bendat, S. & Piersol, A. 1980 *Engineering Applications of Correlation and Spectral Analysis*, Wiley-Interscience

Berkhout, A. J. 1984 'Seismic Resolution: A Quantitative Analysis of Resolving Power of Acoustical Echo Techniques', *Handbook of Geophysical Exploration*, vol. 12, Geophysical Press

Cobo, P., Ranz, C. & Cervera, M. 2002 'Increasing the vertical resolution of conventional sub-bottom profilers by parametric equalisation', *Geophysical Prospecting*, 2002, 50, 139-149

Cobo-Parra, P. & Carbó-Fité, R. 1994 'On the generation of bionic pulses with conventional piezoelectric transducers by proper design of the input driving function', *Journal de Physique IV, colloque C5, supplement au Journal de Physique III*, Volume 4, May 1994

Dragonette, L. R., Numrich, S. K., and Frank, L. J. 1981 'Calibration technique for acoustic scattering measurements', *Journal of the Acoustical Society of America*, vol 69 (4), April 1981

Faran, J. 1951 'Sound scattering by solid cylinders and spheres', *Journal of the Acoustical Society of America*, vol. 23 (4), July 1951

Holly, A. C. 1984 'A method for the generation of broadband acoustic transmissions', *Journal of the Acoustical Society of America*, vol. 75 (3), March 1984

Kaipio, J. & Somersalo, E. 2005 *Statistical and Computational Inverse Problems*, Springer Science+Business Media, New York

Stanton, T. K. & Chu, D. 2008 'Calibration of broadband active acoustic systems using a single standard spherical object', *Journal of the Acoustical Society of America*, vol. 124 (1), July 2008